PROCEEDINGS OF SCIENCE

Solar Cycle Modulation of Cosmic Rays Observed with the Low Energy Modes of the Pierre Auger Observatory

J.J. Masías-Meza[a] **for the Pierre Auger Collaboration**[*,b]

[a] *Departamento de Física and IFIBA, (FCEN-UBA-CONICET), Buenos Aires, Argentina*
[b] *Observatorio Pierre Auger, Av. San Martín Norte 304, 5613 Malargüe, Argentina*
E-mail: auger_spokespersons@fnal.gov
Full author list: http://www.auger.org/archive/authors_2015_06.html

The low energy modes of the surface detector array of the Pierre Auger Observatory record variations in the flux of low energy secondary particles with extreme detail. These two modes consist of recording (1) the rate of signals for energies between $\sim$ 15 MeV and $\sim$ 100 MeV (the Scaler mode) and (2) the calibration charge histograms of the individual pulses detected by each water-Cherenkov station, covering different energy channels up to $\sim$ 1 GeV (the Histogram mode). Previous work has studied the flux of galactic cosmic rays on short and intermediate time scales (i.e. from minutes to weeks) using these low energy modes. In this work, after including a long-term correction to the response of the detectors, we present the first long-term analysis of the flux of cosmic rays using scalers and two energy bands of the calibration histograms. We show its sensitivity to the solar cycle variation and its relation to the solar modulation of cosmic rays for an 8-year period.

The 34th International Cosmic Ray Conference,
30 July- 6 August, 2015
The Hague, The Netherlands

*Speaker.

PoS(ICRC2015)074

1. Introduction

In the interplanetary medium, the transport of high-energy/non-thermal charged particles with Larmor radius comparable to or smaller than the Heliosphere size, is sensitive to solar magnetic activity, mainly due to its effects (on various space-time scales) on several heliospheric properties.

While many of these effects have been studied since the 1960's, mainly using neutron monitors, during the last decade several new particle detectors (such as muon telescopes or the low energy modes of some high energy observatories) have also begun helping us to better understand the physical processes in the heliosphere that affect the propagation of these energetic particles.

In particular, the solar modulation of galactic cosmic rays (GCRs) on time-scales from minutes to several days, has been studied recently using the flux of secondary particles detected by the surface detector array (SD) of the Pierre Auger Observatory [1, 2, 3]. These studies quantified the sensitivity of GCRs to specific transient interplanetary structures for different energies [4].

The Pierre Auger Observatory [5] is located at Malargüe, Argentina (69.3º W, 35.3º S, 1400 m a.s.l.), and was designed for the study of cosmic rays (CRs) at the highest energies. Its SD array consists of 1660 water-Cherenkov detectors (WCD), arranged in a triangular grid with a spacing of 1500 m, distributed over an area of 3000 km^2.

Measurements of low-energy cosmic rays (primary energies from $\sim$ 10 GeV to a few TeV [3]) can be performed at the Pierre Auger Observatory by exploiting two different low energy modes implemented at the Observatory. These produce complementary sets of data [4]: the Scaler and Histogram modes. The Scaler Mode is a particle counter mode. It was implemented in all the detectors of the SD array and these data are recorded for every station every second, reaching typical counting rates of $\sim 1.8 \times 10^8$ counts per minute. From September 2005, it has recorded the number of signals detected above a very low threshold of 3 ADC counts above the station baseline and with an upper cut of 20 ADC counts. This range of ADC counts corresponds to a deposited energy E_d (in the detector volume) between $\approx$ 15 MeV and $\approx$ 100 MeV [2].

The Histogram mode comes from measuring the properties of pulse signals produced by the particles interacting with the water volume. In particular, one-minute histograms are built at each SD station from the peak of each signal (peak histograms), and from the total charge deposited at the photomultiplier tubes (PMTs) of the detectors (charge histograms), which is proportional to the deposited energy within the detector volume [6]. Thus, after a calibration process considering the energy deposited E_d by a central and vertical muon (equivalent to a signal of 1 VEM, for vertical equivalent muon), it is possible to construct histograms of deposited energy up to $\sim$ 1 GeV. The use of histogram data allows us to study the variation of the counting rates in different energy-deposit bins, corresponding to different CR primary energies [4]. There are two particular ranges that will be analyzed in the present paper: one comparable to deposited energies of the scaler mode (E_d between 60 MeV and 120 MeV), and one associated with energies deposited by single muons near the range associated with vertical incidence (E_d between 200 MeV and 280 MeV).

Both Scaler and Histogram modes are complementary in some sense, and so it is also possible to make a cross-check of the two kinds of data for making consistency tests.

By using the data described above, we have studied so far [1, 2, 4, 3] transient phenomena of solar origin such as, for instance, Forbush decreases produced by Interplanetary Coronal Mass Ejections and the daily modulation of the counting rate. In this paper, for the first time, we exploit

these data to study CR variations over time-scales close to that of one solar cycle. The data used in the following span an 8-year period from January 2006 to December 2013.

In section 2 we describe the general data treatment and selection criteria applied to Scaler and Histogram data. In section 2.1, we present the corrections that we apply to the data to take into account the long-term variations of the response of the water-Cherenkov detector to particles. This correction is followed by a data rejection, described in section 2.2, and then we describe (2.3) how we account for atmospheric effects (mainly due to pressure) on the rate of observed particles. Then, in Sections 3 and 4, we show the behavior of the corrected counting rate at different energies and over 8 years, and compare them with neutron-monitor data, giving a discussion and our conclusions for this paper.

2. Data Treatment

It is well established that the so called Area over Peak (AoP) signals characterize the long-term (years) variations of the response of a WCD to particles (see for example [7, 5] and cited references therein). This AoP is a proxy for the impulse response of the detector to individual muons, and is defined as the ratio of the deposited charge ($\mathrm{VEM_q}$) to the peak ($\mathrm{VEM_p}$) of the pulses associated to the passage of vertical muons trough the water volume:

$$\mathrm{AoP} = \frac{\mathrm{VEM}_q}{\mathrm{VEM}_p}. \tag{2.1}$$

As the signals given by extensive air shower detected in the WCD are calibrated in terms of the instantaneous value of the charge corresponding to the VEM [6], these variations do not affect the standard data reconstruction and analysis. Even so, since the data of the low energy modes are based on the detector response to secondary particles produced during the interaction of CRs with the atmosphere, the AoP variation with time could affect the rates measured in those modes and so has to be corrected when long-term solar modulation effects (such as the eleven year solar cycle) are to be studied.

In this section we explore the effect of the AoP evolution as a function of time on the scaler rate and histograms at the individual station level, and then implement a procedure to correct the long-term behaviour for this effect.

The main interest of this work is to analyze the corrected data from the two modes (Scalers and Histograms) and to find the physical long-term flux of atmospheric secondaries as measured by the entire array. To do this, we introduce a particular data analysis process at the individual detector level.

The high statistics of the array allow us to introduce restrictive filters to guarantee the quality of the data we include in this study. We only include data that satisfy the following conditions: 1) the three PMTs of the detector must be operative (this information is obtained by counting the number of working PMTs in the monitoring data as a function of time), 2) the average number of operative detectors must be: 2.a) for scalers: larger than than 600 within 5 minutes intervals; 2.b) for histograms: larger than 150 within 15 minutes intervals; and 3) for histogram data we include an additional criterion: we only use histograms whose first local maximum (the so called

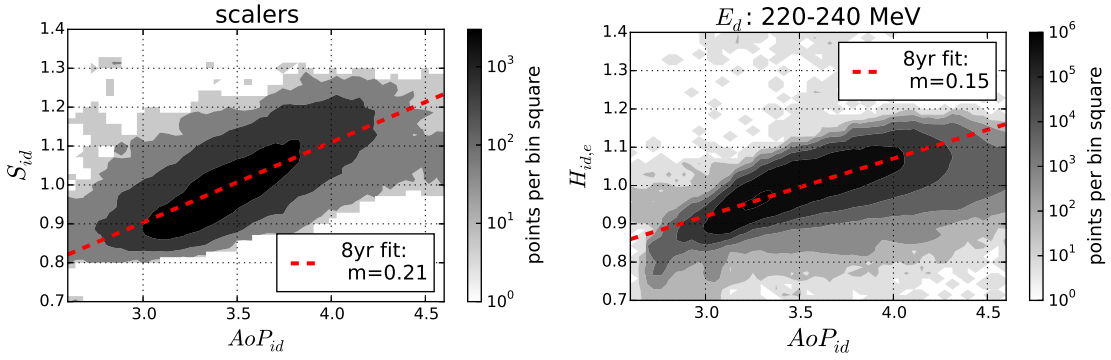

Figure 1: Two dimensional histogram showing the correlations between the Scaler rates S_{id} and AoP_{id} at individual WCD station data. Left panel: using scaler data averaged over 5-day time windows. Right panel: we show the rate, for the band where the muon content is dominant, for charge histograms at 15-min resolution level. This band is shown as an example; for the rest of the energy channels, the correlations have different slopes but similar structures, as shown in figure 2. The bin widths in AoP and the normalized rates are respectively 0.04 and 0.014. The dashed red lines represent the linear fits obtained from equation (2.2).

electromagnetic peak) is located at values of deposited energies larger than 20 MeV. Histograms that do not fulfill this condition are very few but have typically noisier rates and are discarded.

2.1 Area over Peak correction

In the following section we present corrections by looking for linear correlations between AoP and count rates (scaler and histograms) at the individual SD level.

A strong correlation is found when the data from the whole array are considered, as can be seen in Figure 1. These data show that detectors with large AoP values also have large scaler rates. This can be understood since large AoP implies a better response of the detector to individual particles. From the Scaler point of view, larger pulses implies that more pulses will reach the counting threshold to be recorded.

In the following notation, it is understood that S_{id} is the scaler rate of the WCD station with identification number *id*, and that it is normalized by the whole array temporal average $\mathcal{S}^{phys} = \langle\langle S_{id}^{phys}(t)\rangle_{\forall \mathrm{id}}\rangle_{\forall \mathrm{t}}$, such that $S_{id} = S_{id}^{phys}/\mathcal{S}^{phys}$, where the superindex *phys* refers to magnitudes in physical units. Similarly, we will assume that the histograms rates $H_{id,e}$ are normalized by the whole array time average at each energy band E_d indexed with e, denoted by $\mathcal{H}_e^{phys} = \langle\langle H_{id,e}^{phys}(t)\rangle_{\forall \mathrm{id}}\rangle_{\forall \mathrm{t}}$, such that $H_{id,e} = H_{id,e}^{phys}/\mathcal{H}_e^{phys}$. The deposited energy band rates have been processed in uniform intervals of 20 MeV in the range $E_d = (0-1000)$ MeV; so that energy indices are $e = 0, 1, 2, \ldots 49$. To account for the AoP effect we fit a linear regression:

$$\begin{aligned} S_{\mathrm{id}} &= m^{\mathrm{S,AoP}}\mathrm{AoP}_{id} + b^{\mathrm{S,AoP}} \\ H_{\mathrm{id,e}} &= m_e^{\mathrm{H,AoP}}\mathrm{AoP}_{id} + b^{\mathrm{H,AoP}}, \end{aligned} \tag{2.2}$$

obtaining slopes with statistical errors of the order of 1% for scalers and histograms for the 2006–2013 period. The values of $m^{S,AoP}$ and $m_e^{H,AoP}$ are shown in the left panel of Figure 2. The dependence of $m_e^{H,AoP}$ on energy is closely related to the long-term evolution of the charge

histograms. An example of the linear fits for the energy range channel between 220 MeV and 240 MeV is shown in the right side of Figure 1.

To perform a first-order correction in the individual scalers ($S_{\rm id}$) and histograms ($H_{\rm id,e}$), we apply a linear detrend on the individual $\mathrm{AoP}_{\rm id}$ as follows:

$$S_{\rm id}^{\rm corr/AoP}(t) = S_{\rm id}(t) - m^{\rm S,AoP}(\mathrm{AoP}_{\rm id}(t) - \overline{AoP})$$
$$H_{\rm id,e}^{\rm corr/AoP}(t) = H_{\rm id,e}(t) - m_e^{\rm H,AoP}(\mathrm{AoP}_{\rm id}(t) - \overline{AoP}), \quad (2.3)$$

where $S_{\rm id}^{\rm corr/AoP}$ and $H_{id,e}^{corr/AoP}$ are the rates corrected for the AoP modulation. The global average over the considered detectors and the whole time period is given by $\overline{AoP} = \langle\langle AoP_{id}(t)\rangle_{\forall \rm id}\rangle_{\forall \rm t}$. The number of detectors included in the average calculation is not necessarily the whole array, as the detectors must pass the filters mentioned earlier in this section. The average term has been added in order to conserve the mean values: $\langle\langle S_{\rm id}^{corr/AoP}(t)\rangle_{\forall id}\rangle_{\forall t} = 1$, and similarly $\langle\langle H_{\rm id,e}^{corr/AoP}(t)\rangle_{\forall id}\rangle_{\forall t} = 1$.

2.2 Data rejection method

Once we have obtained the mean value for the AoP corrected scalers and bands-of-histogram rates, we need to take into account those outlier values that do not fit within this correction. To do this, we introduce the following data rejection method: we discard all the scalers $S_{\rm id}^{\rm corr/AoP}(t)$ outside $2.5\sigma(t)$ from the mean value $\langle S_{\rm id}(t)\rangle_{\forall \rm id}$, where $\sigma(t)$ is the standard deviation determined from the set of data of the entire array in a 5 minute window centered at time t.

At this point, we note that when averaging over the entire array, the data are still noisy for some time intervals where the number of detectors contributing data is low. Thus, we include additional filtering criteria, to both the Scaler and Histogram rates:

1. for each time bin, using a moving window centered average with a sliding window of 4-months length, we determine the mean and the standard deviation σ_N of the number of working detectors as a function of time. Those periods where the instantaneous number of detectors is not within $\pm 1\sigma_N$ respect to that mean value are discarded; and

2. the instantaneous $\langle \mathrm{AoP}_{\rm id}(t)\rangle_{\forall \rm id}$ value must be inside $\pm 3.3\sigma(t)$ with respect to the mean of the 4-months period.

2.3 Pressure correction

To obtain the physical signal we still have to correct for the atmospheric pressure effect in the flux. This effect is evidenced as the usual anticorrelation, and the linear parameters can be obtained from the fit of a linear function for the flux as the function of atmospheric pressure. The corresponding slopes for the scalers rates, $m^{S,press}$, and for the histograms bands, $m_e^{H,press}$, can be seen in the right panel of Figure 2. After applying this correction we finally obtain the AoP and pressure corrected rates $\langle S_{\rm id}^{\rm corr/AoP}(t)\rangle_{\forall \rm id}^{\rm corr/press}$, $\langle H_{\rm id,e}^{\rm corr/AoP}(t)\rangle_{\forall \rm id}^{\rm corr/press}$, that will be described in the next section.

For discussions hereafter, we will use the abbreviated notation $\widetilde{H}_e^{phys} = \mathcal{H}_e^{phys} \times \langle H_{\rm id,e}^{\rm corr/AoP}(t)\rangle_{\forall \rm id}^{\rm corr/press}$, which refers to histogram rates corrected by AoP and barometric effects, with physical units at each energy band e.

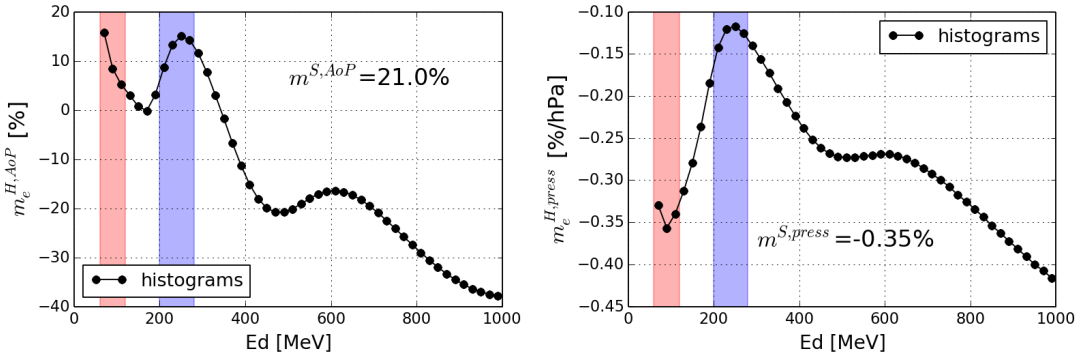

Figure 2: Left: slopes $m_e^{\mathrm{H,AoP}}$ (black dotted lines) from fits to the correlations between charge histogram counts and AoP as shown in Figure 1. Units are in percentage per AoP unit, and the errors are of the order of 1%. In the inset the corresponding unique value for scalers $m^{\mathrm{S,AoP}}$ is shown. Right: slopes $m^{S,press}$ and $m_e^{H,press}$ (black dotted lines) from fits to correlations between histogram rates and atmospheric pressure. As in the left pannel, in the inset the corresponding slope for the Scaler rate with pressure is shown. In both cases, red and blue bands correspond to the H_{sc} and H_{μ} rates, defined in section 3.

3. Results and Discussion

In left panel of Figure 3 we show the long-term pressure-corrected Scaler rates. Grey and black curves show data without and with AoP correction, respectively.

Some differences between the rate of muons and the rate of neutrons (e.g. observed by Neutron Monitors) are known, e.g. due to local atmospheric effects and associated primary energies [8] and because of the different production rates during the shower. However, in the left panel of Figure 3, we present a comparison of observations of the Pierre Auger Scaler mode with data from different neutron monitors (McMurdo, Kiel, and Athens), which have different rigidity cut-offs because of their different geographic locations. Notice that the AoP-corrected Scalers present a global maximum near the middle of 2009, in agreement with the time when neutron monitors observe the maximum flux of GCRs associated with the minimum of solar activity, toward the beginning of the solar cycle 24. As expected, the amplitude of the GCR modulation at different stations decreases monotonically as the geomagnetic rigidity cutoff of each site increases. It should be noted that the rigidity cutoff at Malargüe ($R_c = 9.8$ GV) is well below the characteristic energy of GCRs flux observed with the Scaler mode at Pierre Auger Observatory, which has a median value estimated as ~ 90 GeV (see [3]).

To explore the effects of the solar modulation in different energy ranges, we consider two different channels of deposited energy: low and high energy.

The low energy channel is obtained from integrating the histograms between 60 MeV and 120 MeV of deposited energy, which is related to the scaler trigger bounds and comes from $H_{sc}(t) = \sum_{e=3}^{5} \widetilde{H}_e^{phys}(t) / \sum_{e=3}^{5} \mathcal{H}_e^{phys}$. For this channel we consider limits at E_d =(60-120) MeV because, for energies $E_d \lesssim 60$ MeV, the rate could be affected by the trigger system of the detector.

The high energy channel is related to the second peak of the charge histograms, where vertical muons become the predominant component.It is obtained from $H_{\mu}(t) = \sum_{e=10}^{13} \widetilde{H}_e^{phys}(t) / \sum_{e=10}^{13} \mathcal{H}_e^{phys}$, corresponding to E_d =(200-280) MeV.

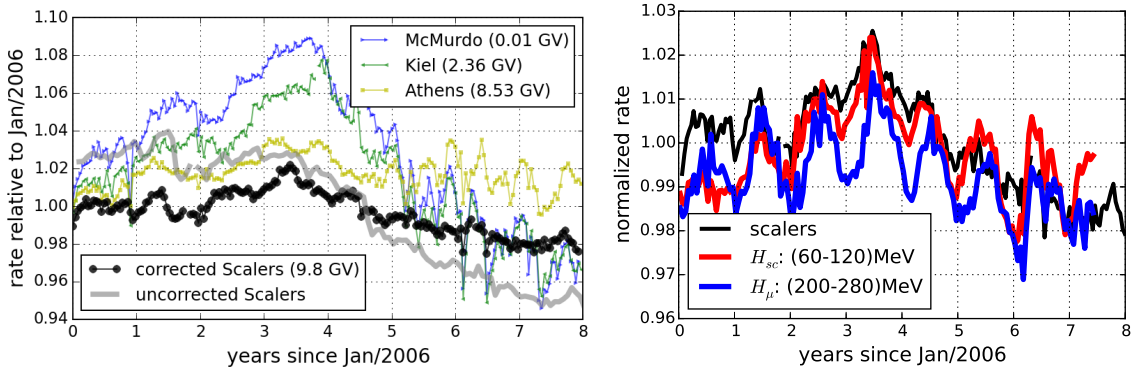

Figure 3: Left panel: Long-term of pressure-corrected Scalers with AoP correction (black dots) and without AoP correction (gray line), compared with different NMs (inset shows geomagnetic rigidity cut-off). The lower Auger amplitude of the solar cycle modulation is consistent with the decreasing trend for high rigidity NMs. Right panel: time profiles for H_{sc} (red) and H_{μ} (blue); both normalized by their time average. In black, the same scaler profile as in left panel. The three profiles show a global peak at the solar minimum period. Note that the global peak at lower energies is stronger than at higher energies, as expected.

The long-term profiles for H_{sc} and H_{μ} are shown in the right panel of Figure 3. In this figure it is also possible to see a global maximum flux of particles near the middle of 2009, at the same time as in the Scalers.

Furthermore, we find that, as expected, the peak at lower energies (H_{sc}) is stronger than at higher energies (H_{μ}). Superposed to the rates of scalers and histograms, there is a pronounced annual modulation, that appears stronger in the Histogram data. This is a negative temperature effect (anticorrelation between the rate and the temperature), an effect that has been previously reported for muon detectors [9, 8]. The increase of the temperature causes a decrease of the air density, and consequently an increase of the volume of the atmosphere; therefore, charged pions are produced higher in the atmosphere and more muons will decay before reaching the detector level.

4. Summary and Conclusions

Summarizing, in the right panel of Figure 3 we present for the first time the long-term (8-years) behaviour for Scalers, for $H_{sc}(t)$, and for $H_{\mu}(t)$, measured by the low energy modes of the Pierre Auger Observatory, where the solar cycle (modulation associated with interplanetary physical mechanisms) and the daily modulation (associated with atmospheric physical processes) can be observed for the different energy bands of these modes.

The period observed corresponds to the last, very weak, period of solar activity, with a consequent interest of being associated with the lowest interplanetary effects on GCRs, ever recorded.

Other detectors that can provide such a long recording period, as the one presented here, are neutron monitors. However, the rates that we present correspond to higher energies than the ones observed using neutron monitors (which also are counters that do not distinguish different energies). Then, our observations can help to better understand the effects of different fundamental

processes (as drift effects or turbulent diffusion) affecting the GCR transport in the heliosphere, for different primary energies.

Furthermore, these low energy mode data (e.g. Scalers, H_{sc}, and H_{μ}) provided by the Pierre Auger Observatory, give the flux of low energy GCRs with the highest statistical significance due to its huge total collecting area from more than 1600 detectors.

Thus, we have presented measurements of scaler and muon fluxes at unprecedented statistical confidence, covering the most interesting period of recent solar cycles. The low energy (scaler and muon) modes of the Pierre Auger Observatory can extend the range of rigidities that are routinely studied using NMs.

References

[1] Asorey H. for the Pierre Auger Collaboration, *Cosmic Ray Solar Modulation Studies at the Pierre Auger Observatory*, *31st International Cosmic Ray Conference*, Lodz, Poland (2009), 41.

[2] Pierre Auger Collaboration, P. Abreu, et al., *The Pierre Auger Observatory scaler mode for the study of solar activity modulation of galactic cosmic rays*, *JINST* **6** (2011), P01003.

[3] Dasso S. and Asorey H., for the Pierre Auger Collaboration, *The scaler mode in the Pierre Auger Observatory to study the heliospheric modulation of cosmic rays*, *Advances in Space Research* **49** (2012), 1563–1569.

[4] Asorey H. for the Pierre Auger Collaboration, *Measurement of Low Energy Cosmic Radiation with the Water Cherenkov Detector Array of the Pierre Auger Observatory*, *32th International Cosmic Ray Conference Beijing* **11** (2011), 467.

[5] Pierre Auger Collaboration, A. Aab et al., *The Pierre Auger Cosmic Ray Observatory*, Accepted for publication in *Nucl. Instrum. Meth. A* (2015) [1502.01323].

[6] X. Bertou and et al, *Calibration of the surface array of the Pierre Auger Observatory*, *Nucl. Instrum. Meth. A* **568** (2006), 839–846.

[7] R. Sato, *Long Term Performance of the Surface Detectors of the Pierre Auger Observatory*, *32th International Cosmic Ray Conference Beijing* **3** (2011), 204.

[8] M. L. Duldig, *Muon Observations*, *Space Sci. Res.* **93** (2000), 207–226.

[9] C. R. Braga, A. Dal Lago, T. Kuwabara, N. J. Schuch, and K. Munakata, *Temperature effect correction for the cosmic ray muon data observed at the Brazilian Southern Space Observatory in São Martinho da Serra*, *Journal of Physics Conference Series* **409** (2013), no. 1.